Simultaneous Surface Plasmon Optical and Electrochemical Investigation of Layer-by-Layer Self-Assembled Conducting Ultrathin Polymer Films

Akira Baba,[†] Mi-Kyoung Park,[‡] Rigoberto C. Advincula,[‡] and Wolfgang Knoll*,[†]

Max-Planck-Institute for Polymer Research, Ackermannweg 10, D-55128 Mainz, Germany, and Department of Chemistry, University of Alabama at Birmingham, Birmingham, Alabama 35294-1240

Received July 13, 2001. In Final Form: March 18, 2002

In this study, we use a novel method for simultaneously measuring the optical and electrochemical properties of layer-by-layer self-assembled conducting ultrathin polymer films. We employed the recently developed combination of in situ surface plasmon resonance spectroscopy (SPS) and surface plasmon field-enhanced light scattering (SPFELS) with an electrochemical method (cyclic voltammetry). Polyaniline (PANI) and sulfonated polyaniline (SPANI) were used as the polycation and the polyanion for the conducting layer-by-layer film assemblies. The doping−dedoping process of the PANI/SPANI at different film thicknesses was investigated by electrochemical-SPS/SPFELS. The potential cycling resulted in characteristic oscillations that were sensitively monitored with this technique. We were able to obtain in situ information on dielectric constant changes of the PANI/SPANI layer-by-layer films with respect to film thickness and their corresponding morphology transitions during the electrochemical process. Thus, this experimental approach allows for the simultaneous elucidation of optical and electrochemical properties of conducting polymers in thin film formats.

Introduction

The layer-by-layer or LbL self-assembly method is a relatively new technique to fabricate molecularly controlled ultrathin multilayer films, as initially reported by Decher et al.[1] The adsorption process involves alternate deposition of polycations and polyanions from solution. By controlling the solution parameters, surface charges, and polymer combination, superlattice and supramolecular structures of alternately charged polymers have been reported.[2] Furthermore, conjugated ultrathin polymer films have also been realized using this alternate self-assembling method.[3,4] The evaluation of the film formation and the electrochemical properties of the layer-by-layer self-assembled conducting polymers is very important.[5] Understanding the properties of these films deposited on a flat electrode surface is of great interest for device applications, such as light-emitting diodes and spectro-electrochemical-based sensors.[6−13]

Surface plasmon resonance spectroscopy (SPS) has been shown to be a technique of high sensitivity for characterizing ultrathin films at the nanometer thickness scale.[14,15] Recently, the combination of SPS with electrochemical techniques for the simultaneous characterization and manipulation of electrode/electrolyte interfaces has been demonstrated.[16,17] The roughness of the metal surface has also been evaluated by monitoring the light scattered off the surface, which was shown to be enhanced by the surface plasmons.[18] Thus, we have been developing a combination of in situ electrochemical/SPS/surface plasmon field-enhanced light scattering (SPFELS) techniques for the investigations of the electrochemical process of polyaniline film formation and the properties of the resulting films on gold metal electrode surfaces.[19]

In this study, the optical/electrochemical properties of ultrathin layer-by-layer polyaniline (PANI)/sulfonated polyaniline (SPANI) films were investigated by cyclic voltammetry with simultaneous monitoring of film properties by SPS/SPFELS. By simultaneously investigating with SPS, we were able to correlate in situ the changes in the dielectric constant and/or film thickness of the PANI/

* To whom correspondence should be addressed. E-mail: knoll@mpip-mainz.mpg.de. Fax: +49-6131-379-360.

[†] Max-Planck-Institute for Polymer Research.

[‡] University of Alabama at Birmingham.

(1) Decher, G.; Hong, J. D. *Makromol. Chem. Makromol. Symp.* **1991**, *46*, 321.

(2) Decher, G. *Science* **1997**, *277*, 1232.

(3) Ferreira, M.; Cheung, J. H.; Rubner, M. F. *Thin Solid Films* **1994**, *244*, 806−809.

(4) Ferreira, M.; Rubner, M. F. *Macromolecules* **1995**, *28*, 7107−7114.

(5) Knoll, W. *Curr. Opin. Colloid Interface Sci.* **1996**, *1*, 137.

(6) Ferreira, M.; Rubner, M. F. *Mater. Res. Soc. Symp. Proc.* **1994**, *328*, 119.

(7) Fou, A. C.; Onitsuka, O.; Ferreira, M.; Rubner, M. F. *Mater. Res. Soc. Symp. Proc.* **1995**, *369*, 575−580.

(8) Onoda, M.; Yoshino, K. *J. Appl. Phys.* **1995**, *78*, 4456.

(9) Tian, J.; Wu, C.-C.; Thompson, M. E.; Stum, J. C.; Marcella, M. J.; Swager, T. M. *Adv. Mater.* **1995**, *7*, 395−397.

(10) Hong, H.; Davidov, D.; Avany, Y.; Chayet, H.; Faraggi, E. Z.; Neumann, R. *Adv. Mater.* **1995**, *7*, 846−849.

(11) Ho, P. K. H.; Kim, J.-S.; Burroughes, J. H.; Becker, H.; Li, S. F. Y.; Brown, T. M.; Cacialli, F.; Friend, R. H. *Nature* **2000**, *404*, 481−484.

(12) (a) Advincula, R.; Frank, C. W.; Roitman, D.; Sheats, J.; Moon, R.; Knoll, W. *Mol. Cryst. Liq. Cryst.* **1998**, *316*, 103−112. (b) Advincula, R. C.; Knoll, W.; Frank, C. W.; Roitman, D.; Moon, R.; Sheats, J. *Mater. Res. Soc. Symp. Proc.* **1998**, 115−120.

(13) (a) Mark, H.; Rubinson, J. F. Conducting Polymer Films as Electrodes. In *Interfacial Electrochemistry; Principles and Applications*; Wieckowski, A., Ed.; Marcel Dekker: New York, 1999; pp 839−841. (b) Seliskar, C.; Ross, S.; Slaterbeck, A.; Shi, Y.; Aryal, S.; Maizels, M.; Heineman, W.; Ridgway, T.; Nevin, J. *Proc. SPIE* **1999**, *3537*, 268−279. Slaterbeck, Y.; Shi, S.; Aryal, M.; Maizels,W. R.; Heineman, T. H.; Ridgway, T.; Nevin, J. H. (c) Ross, S.; Seliskar, C.; Heineman, W. *Anal. Chem.* **2000**, *72*, 5549−5555.

(14) Knoll, W. *Annu. Rev. Phys. Chem.* **1998**, *49*, 569.

(15) Advincula, R.; Aust, E.; Meyer, W.; Knoll, W. *Langmuir* **1996**, *12*, 3536.

(16) Chinowsky, T. M.; Saban, S. B.; Yee, S. S. *Sens. Actuators, B* **1996**, *35−36*, 37.

(17) Badia, A.; Arnold, S.; Scheumann, V.; Zizlsperger, M.; Mack, J.; Jung, G.; Knoll, W. *Sens. Actuators, B* **1999**, *54*, 145.

(18) Fontana, E.; Pantel, R. H. *Phys. Rev. B* **1988**, *37*, 3164.

(19) (a) Baba, A.; Advincula, R.; Knoll, W. *PMSE Prepr.* **2001**, *84*, 674. (b) Baba, A.; Advincula, R.; Knoll, W. *J. Phys. Chem. B* **2002**, *106*, 1581. (c) Xia, C.; Advincula, R.; Baba, A.; Knoll, W. *Langmuir* **2002**, *18*, 3555.

10.1021/la011078b CCC: $22.00
Published on Web 05/17/2002

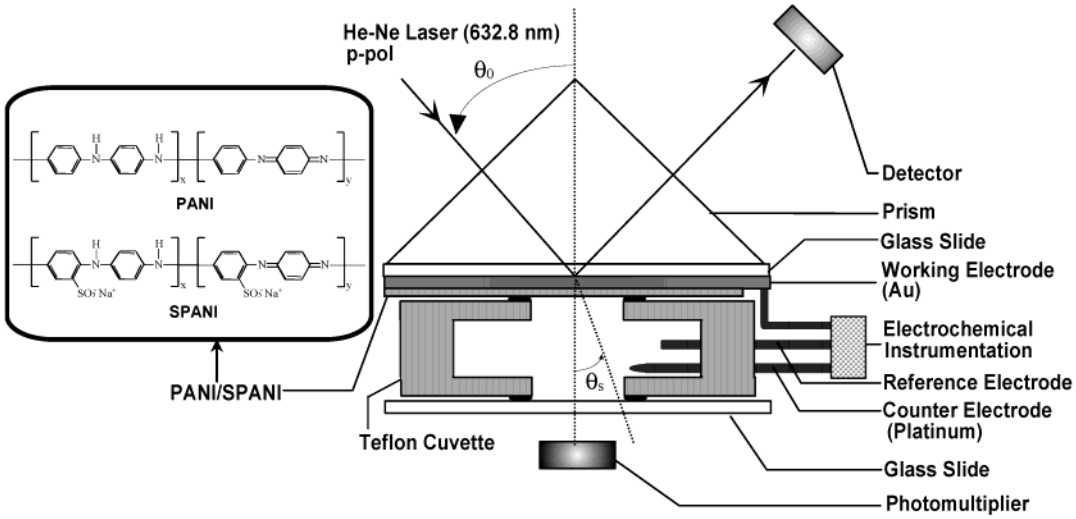

Figure 1. ATR setup for the excitation of surface plasmons in the Kretschmann geometry (a thin metal film is evaporated onto the base of a glass prism and acts as a resonator driven by the photon field) and structural formulas of the employed PANI and SPANI.

SPANI during the doping−dedoping or protonation−deprotonation processes. The incident light enhanced by surface plasmons and scattered off the substrate/electrode interface also enabled us to investigate the changes in roughness of the PANI/SPANI films upon the potential cycling.

Experimental Section

Materials. The chemical structures of the polyelectrolyte materials employed in the experiments are shown in Figure 1. The synthesis of PANI and SPANI follows the procedures of MacDiarmid[20] and Epstein,[21] respectively. The initially synthesized emeraldine hydrochloride was converted to emeraldine base by reacting with NH_4OH, ammonium hydroxide for 24 h. The polymer can be made water-soluble according to a procedure of Rubner et al.[22] as a dilute solution by first dissolving it in DMAc, dimethylacetamide, 20 mg/mL, and subsequent dilution 1:10 in water (pH 3.0−3.3). Then the pH was adjusted to around pH 2.6. Sulfonation of PANI proceeded by reacting with fuming sulfuric acid and isolating the product, which was very soluble in 0.1 M NaOH. The pH of the SPANI solution was adjusted to around pH 3.0 before use.[4] The MW was estimated to be between 25 000 and 50 000 on the basis of a similar literature procedure. Poly(allylamine hydrochloride) (PAH; MW 50 000−65 000) and poly(sodium 4-styrenesulfonate) (PSS; MW 70 000) were obtained from Aldrich. 3-Mercapto-1-propanesulfonic acid, sodium salt, and (3-aminopropyl)triethoxysilane (APS) for gold and glass slide substrate functionalizations, respectively, were also obtained from Aldrich.

Layer-by-Layer Adsorption. The layer-by-layer adsorption of the polyanion and the polycation was performed following the Decher approach.[23,24] The gold surface of the flat solid substrate was functionalized by immersion of the slide for 1 h in an ethanol solution of 3-mercapto-1-propanesulfonic acid, sodium salt (0.001 M) (followed by rinsing), creating a uniformly charged (negative) substrate surface. The gold film with a thickness of ∼50 nm was deposited by vacuum evaporation onto a BK7 glass slide with a 1−2 nm thick chromium adhesion layer. The thiol/Au/Cr/glass substrates were then immersed for a few seconds in dilute HCl solution prior to the layer-by-layer adsorption. The bare glass substrates were functionalized by APS (0.1% in acetone). The APS layer was charged by immersion in dilute HCl solution and used immediately for preparing the layer-by-layer ultrathin film. The Au/Cr/glass or glass substrates with the functionalized surfaces were alternately immersed for 15 min in aqueous solutions of the polycation and the polyanion until the desired layer number was achieved. This immersion time is typical for most procedures reported in the literature.[24,25] Rinsing with deionized water at pH 5.6 (Milli-Q, 18 MΩ) was done between depositions. Aqueous solutions of PAH and PSS were prepared with a concentration of 0.001 M per repeat unit. The deposition of the polyelectrolyte layers was carried out using a HMS Series Programmable Slide Stainer apparatus (Carl Zeiss, Inc.) with a 15 min immersion time involving rinsing steps in between.

Electrochemical Measurement. Electrochemical experiments were performed in a conventional three-electrode cell with the Au/Cr/glass substrate as the working electrode, a platinum wire as the counter electrode, and an Ag/AgCl (3 M NaCl) reference electrode. A potentiostat (Princeton Applied Research 263A, EG&G) was used for the cyclic voltammetry experiments.

Electrochemical SPS/SPFELS. Figure 1 shows the attenuated total reflection (ATR) setup used for the excitation of surface plasmons in the Kretschmann configuration combined with an electrochemical cell. A LaSFN9 prism was used. The Au/Cr/glass substrates were clamped against the Teflon cuvette with an O-ring providing a liquid-tight seal. The cuvette was then mounted to the two-axis goniometer for investigations by SPR. Details of this setup have been described previously.[19,26] Surface plasmons are excited at the metal/dielectric interface, upon total internal reflection of polarized He−Ne laser light (λ = 632.8 nm). The optical/electrochemical processes on the gold were detected in situ by monitoring reflectivity changes as a function of time at a fixed incident angle θ_0. Light scattering due to the roughness of the electrode and/or deposited film enhanced by surface plasmons, $dI_s/I_0\, d\Omega$, was detected by the photomultiplier detector at a fixed angle of observation θ_{obs}. $\theta_s = 0$ (vertical to the glass slide) for in situ investigation during the potential cycling of a layer-by-layer conducting film at the planar metal electrode/electrolyte interface.

Results and Discussion

PANI/SPANI Layer-by-Layer Assembly. A sequence of reflectivity data (SPS) and light scattering data (SPFELS) was taken after each polyelectrolyte double-layer deposition, as shown in Figure 2. These scans were measured in ambient air. Shifts of the dip angles of SPS

(20) MacDiarmid, A.; Chiang, J.; Richter, A.; Somasiri, N. In *Conducting Polymers*; Alcacer, L., Ed.; D. Reidel Publishing: New York, 1987; p 105−120.
(21) Epstein, A. J.; Yue, J. *J. Am. Chem. Soc.* **1990**, *112*, 2800.
(22) Cheung, J. H.; Stockton, W. B.; Rubner, M. F. *Macromolecules* **1997**, *30*, 2712.
(23) Decher, G.; Hong, J. D. *Ber. Bunsen-Ges. Phys. Chem.* **1991**, *95*, 1430.
(24) Advincula, R. *IEICE Trans. Electron.* **2000**, *7*, 1104.
(25) Baba, A.; Kaneko, F.; Advincula, R. C. *Colloids Surf., A* **2000**, *173*, 39.
(26) Aust, E. F.; Ito, S.; Sawondny, M.; Knoll, W. *Trends Polym. Sci.* **1994**, *2*, 9.

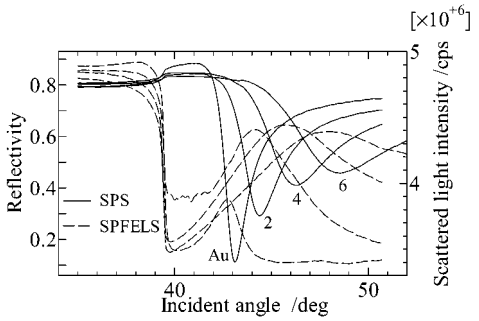

Figure 2. Series of angular SPS curves and surface plasmon field enhanced light scattering (SPFELS) curves taken after each polyelectrolyte double-layer deposition.

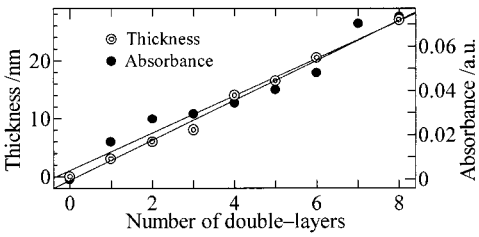

Figure 3. Plots of the thickness and the absorbance at $\lambda = 633$ nm as a function of double-layer number.

and of the peak angles of SPFELS were observed with increasing number of layers. The intensity of the light scattered for the PANI/SPANI film was observed to be higher than that of the bare gold.

The scattered light intensity for bare gold is due to the inherent surface roughness (characteristic of the deposition process). For the PANI/SPANI layer-by-layer film, it can be attributed to roughness contributions from the gold/[PANI/SPANI] film and [PANI/SPANI]/air interfaces. Since we observed the superposition of scattered light between the two interfaces in the case of the PANI/SPANI film, the intensity was higher and the peak broader than those of bare gold. Increasing the number of layers resulted in broader and shallower peaks so that the enhancement of the electric field due to excitation of surface plasmons was decreased with increasing number of layers. However, the peak intensities of the scattered light for the PANI/SPANI films were about the same at each successive double layer. We believe that the observed scattered light intensities can be attributed not only to the roughness of the interfaces gold/[PANI/SPANI] and [PANI/SPANI]/air but also to combinations originating from internal interfaces of the PANI/SPANI layers. This result indicates that the continued deposition of PANI/SPANI films leads to an increasing roughness and inhomogeneity consistent with previous reports.[3,4,12,22]

Figure 3 shows plots of the thickness and of the absorbance at $\lambda = 633$ nm as a function of the double-layer number. A linear behavior was observed. The thickness of one double-layer was calculated to be 3.4 nm by a Fresnel algorithm. The complex dielectric constant $\epsilon_r + i\epsilon_i$ of the layer-by-layer PANI/SPANI film was determined to be 2.2 + i0.66, using the value of the absorbance at $\lambda = 633$ nm obtained from UV−vis spectroscopy. Again, the properties of the PANI/SPANI layer-by-layer assemblies were similar to those reported in previous papers.[12,13]

Electrochemical SPS/SPFELS. Figure 4 shows the cyclic voltammogram and SPS and SPFELS data of four double-layers of PANI/SPANI in 0.5 M H_2SO_4 solution during potential cycling from −0.2 to 0.9 V at the scan rate 100 mV s^{-1}. The solid line shows the cyclic voltammogram, the dashed line shows the SPS curve, and the dotted line shows the SPFELS curve, respectively. As reported by others,[27−29] the first redox process (at 0.22 V in the anodic scan and 0.13 V in the cathodic scan) corresponds to anion transport, that is, anion doping and dedoping, from the electrolyte solution to the PANI/SPANI film. The second redox process (ca. 0.8 and 0.75 V, respectively) simply corresponds to the imine nitrogen deprotonation and protonation; that is, protons in the PANI/SPANI film are expelled into the electrolyte solution and inserted into the polyaniline film, respectively. The anion is also inserted during the protonation of the PANI/SPANI film and expelled from the film during the deprotonation as a counterion to the iminium cation formation (doping).

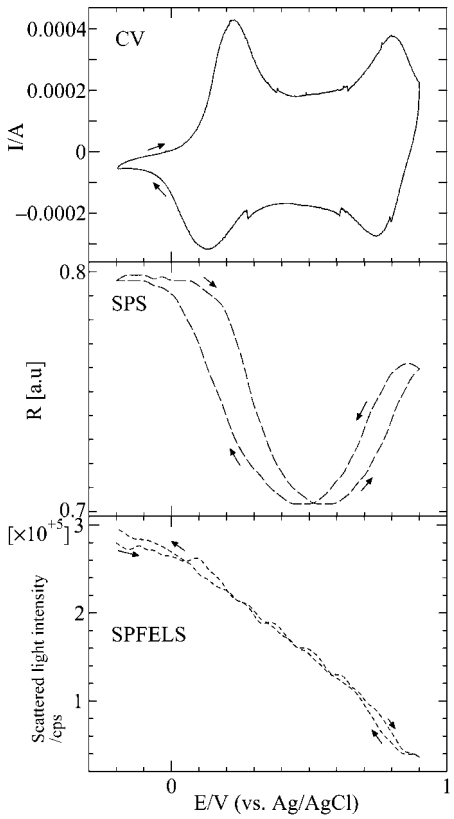

Figure 4. Simultaneous observation of the cyclic voltammmogram, SPS curve, and SPFELS curve of four double-layers of the PANI/SPANI film during the potential cycling in 0.5 M H_2SO_4 solution at the scan rate 100 mV s^{-1}.

The SPS reflectivity decreases during doping by the anion and increases during dedoping of anion for the deposited PANI/SPANI, respectively. Moreover, an increase of the SPS during the deprotonation and a decrease during the protonation can be observed in the anodic and the cathodic scans, respectively. In the experiment using the electrochemical quartz crystal microbalance (E-QCM), Orata et al. observed an increase in the film mass by the doping and a decrease in the film mass by the dedoping of the ion.[28] This can be associated with changes in the density of the film or in its thickness. However, in our SPS measurements, the SPS reflectivity was observed to decrease by the doping with the ion. Normally, if it is measured at the low angle slope of the reflectivity curve,

(27) Orata, D.; Buttry, D. A. *J. Am. Chem. Soc.* **1987**, *109*, 3574.
(28) Huang, W. S.; Humphrey, B. D.; MacDiarmid, A. G. *J. Chem. Soc., Faraday Trans.* **1986**, *1*, 82.
(29) Daifuku, H.; Kawagoe, T.; Yamamoto, N.; Ohsaka, T.; Oyama, N. *J. Electroanal. Chem.* **1989**, *274*, 313.

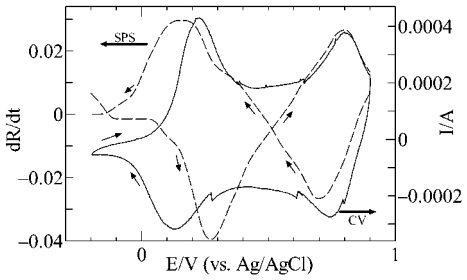

Figure 5. Time differential SPS curve (d*R*/d*t*) as a function of potential cycling between −0.2 and 0.9 V at the scan rate 100 mV s^{-1} and the cyclic voltammogram in 0.5 M H_2SO_4 (four double-layers of the PANI/SPANI film).

an increase in SPS reflectivity is related to an increasing thickness, assuming a constant refractive index.[14,26] In this case we believe that the dielectric constant plays a larger role in the observed SPS reflectivity behavior.

Figure 5 shows the time differential SPS curve and the cyclic voltammogram of a four-double-layers PANI/SPANI film at the scan rate 100 mV s^{-1}. It can be clearly seen that the d*R*/d*t* curves decreased during the anion doping and increased during the anion dedoping process. The d*R*/d*t* curve shows a delay compared with the oxidation peaks of the polyaniline film during the doping process (0.27 V) in the first redox process but changes its slope earlier than the CV peak during the dedoping process (0.16 V).

From the above observations, three possible explanations for the change of the SPS curve by the anion doping−dedoping process can be considered. This includes the *thickness change*, Δd, of the PANI/SPANI film by anion doping−dedoping and the other two, the dependence of the reflectivity curves on *different dielectric constants*, ϵ_r and ϵ_i. If the change in thickness of a PANI/SPANI film is the main component of the SPS curve change, the reflectivity should increase during doping (if measured at angles lower than the resonance) because the insertion of the anion and, simultaneously, of water molecules into the PANI/SPANI film will result in film swelling. This was not observed in our data. Therefore, we believe that the change of the SPS curve in Figures 4 and 5 is dependent primarily on the change of the dielectric constants, ϵ_r and ϵ_i, of the PANI/SPANI film and not on the change of its thickness. This finding then indicates that the dielectric constant of the PANI/SPANI film *decreases* upon ion doping and increases upon ion dedoping. These observations are consistent with a tradeoff between the Δn and Δd components of the SPR data.[14,26] We consider this to be consistent with the E-QCM data by Orata[28] where ion doping results in an increase in film mass and density (insertion of ions and protonation), thereby decreasing the dielectric constants but not necessarily increasing the optical thickness of the film as monitored by SPR.

Repeated Potential Cycling. Figure 6 shows the simultaneous observation of the current, the reflectivity, and the SPFELS data, respectively, upon potential cycling of the four-double-layers PANI/SPANI film up to four cycles in 0.5 M H_2SO_4 solution at the scan rate 100 mV s^{-1}. These plots are helpful in understanding the mechanism of the electrochemical redox behavior with repeated potential cycles. The lifetime of the PDDA (poly(diallyldimethylammonium chloride))/SPANI film was reported recently by Sarkar and Ram et al.[30] to be better than 10^5 cycles.

(30) Sarkar, N.; Ram, M. K.; Sarkar, A.; Narizzano, R.; Paddeu, S.; Nicolini, C. *Nanotechnology* **2000**, *11*, 30−36.

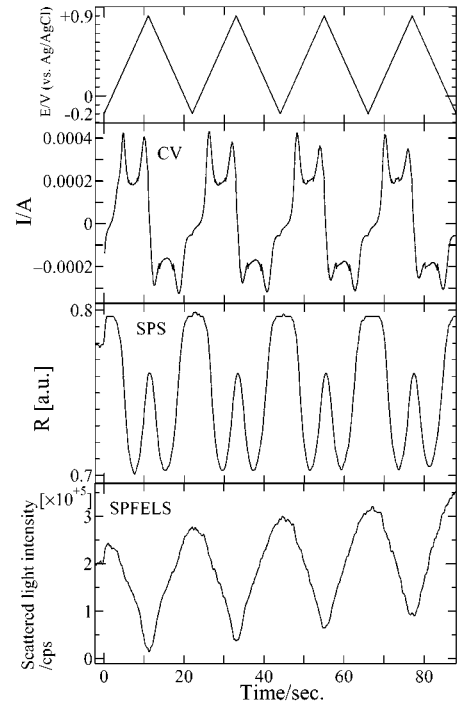

Figure 6. Simultaneous observation of current, SPS, and SPFELS of four double-layers of the PANI/SPANI film in 0.5 M H_2SO_4 solution as a function of potential cycling at the scan rate 100 mV s^{-1}. Top: potential ramp vs time.

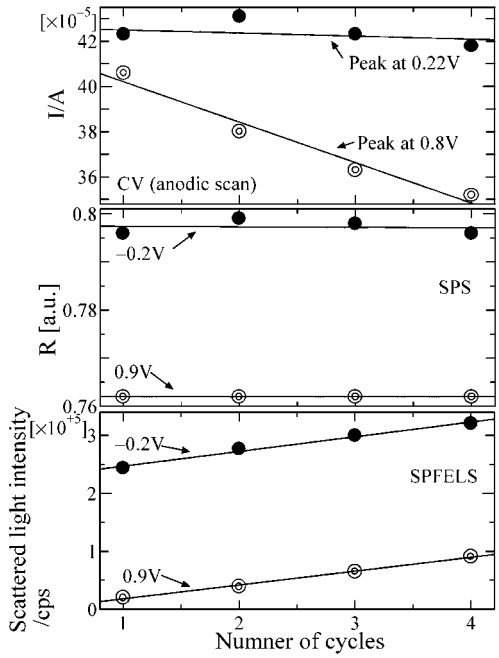

Figure 7. Plots of the peak current, the SPS, and the SPFELS as a function of cycle number.

The top panel in Figure 6 shows the potential ramp versus time. The current and the SPS curves have almost similar onset values and magnitudes (*y*-axis) at each potential cycling. This implies that the changes of the dielectric constant of the PANI/SPANI film at each potential cycling are identical and reversible. However, the repeated potential cycling resulted in a gradual increase in the scattered light intensity of the SPFELS curve (*y*-axis values). This observation reveals that repeated potential cycling slightly increases the roughness of the surface of the PANI/SPANI film. This is clearly seen in plots of the peak current for SPS and SPFELS,

respectively, at each cycle (Figure 7). As shown in this plot, the peak current for the second redox process (0.8 V) decreases with potential cycling. We believe that the increasing roughness by repeated potential cycling is the main reason for the decrease during the second redox process. This is mainly due to a subsiding deprotonation−protonation process because the peak current of the anion doping−dedoping process in the first redox process (0.22 V) remains largely constant. The subsiding process could be attributed to a decreasing availability of imine nitrogens on the PANI/SPANI film as a result of changing polymer conformation or film morphology with each succeeding cycle.[19,28,30] Furthermore, it is clear that the optical properties, that is, thickness and dielectric constant of the PANI/SPANI film, are constant with repeated potential cycling, as observed from the SPS data. Note that the light scattering enhanced by surface plasmons is sensitively changed by surface roughness even if there is no change in the SPS property.[19] These observations and interpretations clearly identify the uniqueness of this experimental setup in distinguishing the doping and dedoping properties from the deprotonation and protonation processes. Further studies are underway to investigate potential cycling with various electrochemical conditions, for example, solvents, ions, concentration, and so forth.

Conclusions

Our studies have demonstrated the possibilities of performing a combination of in situ surface plasmon resonance spectroscopy (SPS) and surface plasmon field enhanced light scattering (SPFELS) experiments together with cyclic voltammetry for the investigation of the electrochemical processes of layer-by-layer assembled conducting ultrathin polymer films on flat electrode substrates. Potential cycling resulted in sensitive oscillations of the SPS curve. In particular, the time differential SPS curve could be correlated with the cyclic voltammogram. The light scattering enhanced by the surface plasmon also demonstrated the changes in the roughness of the PANI/SPANI film during repeated potential cycling. This allowed for a distinction between the deprotonation−protonation and the doping−dedoping processes in these films. Thus, these results indicate that the simultaneous observation with surface plasmon optical techniques and the cyclic voltammogram allows for the sensitive elucidation of the optical, electrochemical, and roughness properties of layer-by-layer films of conducting polymers.

Acknowledgment. We are grateful to Prof. J. Lipkowski of the University of Guelph for helpful discussions. A.B. would like to acknowledge the Alexander von Humboldt Foundation for a postdoctoral fellowship. R.C.A. and M.P. would like to acknowledge partial support from NSF-CAREER Grant DMR-99-82010.

LA011078B